Solid State Ionics xxx (2015) xxx–xxx

Contents lists available at ScienceDirect

Solid State Ionics

journal homepage: www.elsevier.com/locate/ssi

H/D isotope effects in high temperature proton conductors

N. Bonanos [a], A. Huijser [a,b], F.W. Poulsen [a]

[a] Department of Energy Conversion and Storage, Technical University of Denmark, Risø Campus, P.O. Box 49, DK-4000 Roskilde, Denmark
[b] Optical Sciences group, MESA + Institute for Nanotechnology, University of Twente, P.O. Box 217, 7500 AE, Enschede, The Netherlands

ARTICLE INFO

Article history:
Received 17 December 2014
Received in revised form 13 March 2015
Accepted 14 March 2015
Available online xxxx

Keywords:
Proton conductor
Isotope effect
Hydrogen
Deuterium
Tritium
Zero point energy

ABSTRACT

The atomic mass ratio of *ca.* 2 between deuterium and hydrogen is the highest for any pair of stable isotopes and results in significant and measurable H/D isotope effects in high temperature proton conductors containing these species. This paper discusses H/D isotope effects manifested in O–H/O–D vibration frequencies, the mobility of H^+/D^+ carriers, the kinetics of the electrochemical oxidation of H_2/D_2, the solubilities of H_2O/D_2O and, finally, the spontaneous electromotive force that appears across H_2/D_2 cells with proton conducting electrolytes. Comparable work on tritium-exchanged materials is also discussed. The results highlight the usefulness of isotope effects in the study of high temperature proton conductors.

1. Introduction: hydrogen and deuterium

The masses of hydrogen, deuterium and tritium are in the ratio 1/2/3, the largest for any set of isotopes.[†] Deuterium is stable, while tritium decays to ^3He with a half-life of 12.3 years releasing an electron. The mass difference does not noticeably affect the electronic structure of compounds formed by these species, but does affect their vibrational frequencies in the infra-red, and also the vibrational entropy of the compounds. As a result, the physical and chemical properties are affected, exemplified by the slightly higher vapour pressure of H_2O compared to D_2O[‡] and a difference in the ionisation constants of the liquids [1]. Isotopic substitution also affects the length of hydrogen bonds [2]. The difference in Gibbs free energy of the reaction $2H_2 + O_2 \leftrightarrows 2H_2O$ and the corresponding one for D_2 and D_2O is noticeable in an electrochemical cell. For example, the theoretical electromotive force (emf) of a cell with D_2/D_2O (1%) vs. H_2/H_2O (1%) with an oxide ion conducting solid electrolyte can be calculated from thermodynamic data [3], in the temperature range 800 to 1200 K, resulting in Eq. (1):

$$E = -30.55 + 0.0128 \cdot T \quad (1)$$

where E is in mV and T in K. For the temperature range considered, the D_2/D_2O side is negative.

In high temperature proton conductors (HTPCs), the hydrogen species exist primarily as $OH^{\bullet}$ (Kröger–Vink notation) occupying oxide ion sites [4–6]. The hydrogen in the $OH^{\bullet}$ species is derived from water vapour via reaction Eq. (2). This reaction depends on the presence of oxide ion vacancies, which are usually introduced by doping with an element of lower valence. When the oxide is fully protonated, the $OH^{\bullet}$ concentration is determined by the doping level.

$$H_2O\,(g) + V_O^{\cdot\cdot} + O_O^{\times} \leftrightarrows 2\,OH_O^{\cdot}. \quad (2)$$

A mechanism for proton incorporation that does not rely on water vapour is reaction (3) [7–9]. However, as it involves the creation of electronic defects, it is less favourable energetically. As demonstrated by a defect modelling study [10], reactions (2) and (3) are not mutually exclusive.

$$H_2(g) + 2\,O_O^{\times} \leftrightarrows 2\,OH_O^{\cdot} + 2\,e'. \quad (3)$$

Isotope effects are the changes in the physical or chemical properties resulting from isotopic substitution. HTPCs offer several illustrations of such effects, including changes in the concentration and ionic mobility of the protons and in the electrode kinetics of hydrogen oxidation. This work draws these effects together in the hope of promoting their better understanding. Examples are provided from the subgroup of perovskite proton conductors [11]. The points raised apply also to other HTPCs, but not to the class of low temperature proton conductors, where mostly vehicular transport mechanisms operate [12,13].

E-mail address: nibo@dtu.dk (N. Bonanos).

[†] The masses of H, D, and T are 1.007825, 2.013553, and 3.01605 amu respectively.

[‡] For example, at 10 °C, the vapour pressure of H_2O is 20% higher than that of D_2O.

http://dx.doi.org/10.1016/j.ssi.2015.03.028
0167-2738/

2. Isotope effects in perovskite proton conductors

2.1. Infra-red spectra

In the classical treatment of the O–H and O–D bonds as harmonic oscillators, the ratio of their vibration frequencies is determined by the reduced masses, m^*, of the two systems, assuming that the O atoms are unconstrained. Eqs. (4) to (6) describe these phenomena.

$$\frac{\omega_{O-H}}{\omega_{O-D}} = \sqrt{\frac{m^*_{O-D}}{m^*_{O-H}}} \tag{4}$$

where

$$m^*_{O-H} = \frac{m_O m_H}{m_O + m_H} \tag{5}$$

and

$$m^*_{O-D} = \frac{m_O m_D}{m_O + m_D}. \tag{6}$$

For ^{16}O–^{1}H and ^{16}O–^{2}D, this ratio comes to $\sqrt{17/9}$, i.e. 1.374. For an H/D species attached to an infinite mass, the corresponding ratio would be $\sqrt{2}$, i.e. 1.414.

Infra-red spectroscopic studies of D_2O vapour-exchanged perovskites and the perovskite-related structure $LiNbO_3$ showed a systematic shift in the O–D vibration peaks towards lower frequencies/wavenumbers [14–16]. Peaks associated with surface-bound protons were excluded from these studies. Fig. 1 shows the infra-red spectrum for the HTPC $La_{0.8}Sr_{0.2}ScO_{0.95}$ [14]. From the above works, the mean shift of sixteen peaks covering a total of nine compounds was found to be 1.343 ± 0.018, reasonably close, but not identical, to the value calculated based on the reduced mass.

2.2. Protonic conduction

The theories concerning the isotope effect and protonic conduction have been described in an important paper by Nowick and Vaysleyb [17]. The classical model predicts that the rate of a proton hopping in an oxide is proportional to the attempt frequency or O–H vibration frequency. Thus, the mobility of a proton should be larger than that of a deuteron by factor in the range 1.374 to 1.414, while the activation energies of the two species should be identical. These predictions do not agree with observations, therefore this model is discussed no further.

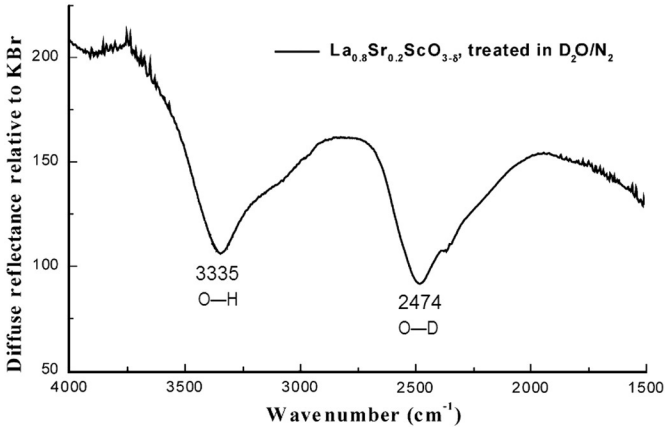

Fig. 1. Infra-red spectrum of HTPC $La_{0.8}Sr_{0.2}ScO_{3-d}$ treated in N_2/D_2O. Peaks for O–H and O–D are clearly resolved [14]. Note the presence of shoulders on the low wavenumber side of the peaks.

The so-called semi-classical treatment modifies the above model by considering the zero-point energy of the H/D species in the potential well in which they reside (Fig. 2). The zero-point energies are given by Eqs. (7) and (8), in which ν_H and ν_D are vibrational frequencies.

$$E_{0,H} = \frac{1}{2}h\nu_H \tag{7}$$

$$E_{0,D} = \frac{1}{2}h\nu_D. \tag{8}$$

The higher vibrational frequency of H results in a higher zero-point energy and, consequently, a lower energy barrier. Taking the mean of the frequencies reported in Refs. [14–16] results in a difference of 5.2 kJ mol^{-1} (0.054 eV), which should be reflected in the activation energies for migration. As for the pre-exponentials of the conductivity, these should be higher for protons than deuterons by a factor of 1.374 to 1.414, the latter value being usually quoted.

Nowick and co-workers assembled conductivity data on fifteen HTPC systems [15–17]. The average difference in activation energy was 4.3 kJ mol^{-1} (0.044 eV), 20% lower than that predicted by semi-classical theory. The discrepancy between observation and theory can be rationalised by recalling that the mechanism of proton transfer between oxygens is not one of simple hopping, but involves the vibrations and librations of the oxygen, as shown by Münch and Kreuer [18,19]. In effect, the barrier "seen" by the proton is modulated by the movements of the oxygen lattice.

In contradiction to the semi-classical model, experimentally determined conductivity pre-exponentials are mostly higher for the D_2O-exchanged HTPCs, in some cases by as much as 1.72. The pre-exponential of the ionic conductivity is described by the following equation [17]:

$$A = \frac{z\lambda^2 e^2 \nu_0 c_{eff}}{6\upsilon k} \tag{10}$$

where

z	is the number of jump directions
λ	is the jump distance
e	is the electronic charge
ν_0	is the vibration frequency
υ	is the unit cell volume
k	is the Boltzmann constant
c_{eff}	is the effective concentration of carriers, allowing for association.

Inspection of Eq. (10) suggests that, apart from ν_0, c_{eff} is the only parameter with the freedom to vary significantly between H and D. Therefore, the inequalities $A_D > A_H$ and $\nu_{0,\,D} < \nu_{0,\,H}$, taken together, lead to the conclusion $c_{eff,\,D} > c_{eff,\,H}$, as pointed out earlier by others [20].

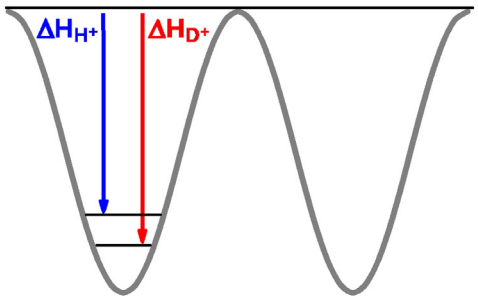

Fig. 2. Semi-classical picture of proton and deuteron in a finite potential well, adapted from Ref. [17]. The different zero-point energies of the two species results in an activation energy for D^+ migration that is higher than that for H^+.

Please cite this article as: N. Bonanos, et al., H/D isotope effects in high temperature proton conductors, Solid State Ionics (2015), http://dx.doi.org/10.1016/j.ssi.2015.03.028

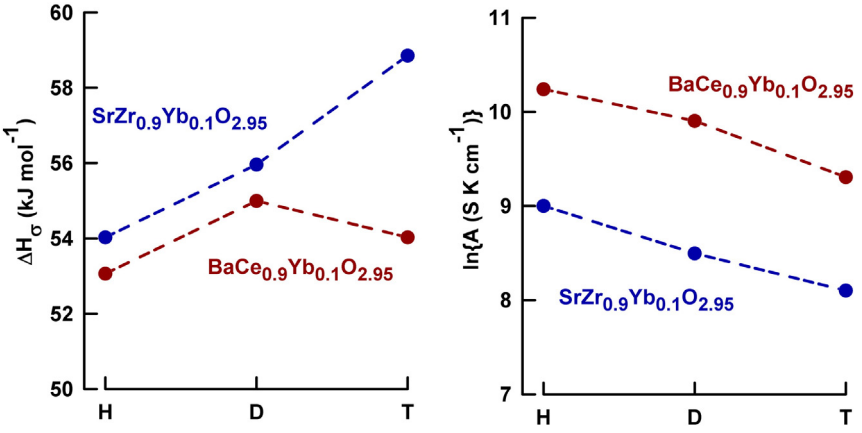

Fig. 3. Arrhenius conductivity parameters in HTPCs exchanged with the three isotopes of hydrogen, based on the data in Ref. [21]. The activation energies increase with isotope mass, except for one point for $BaCe_{0.9}Yb_{0.1}O_{2.95}$, while the pre-exponentials decrease, contrary to expectations from Ref. [17].

Subsequent studies have confirmed the trends found by Nowick in D_2O-exchanged systems, with the exception of one study, which is noteworthy because it also involved T_2 exchange [21]. In this study, the perovskites $SrZr_{0.9}Yb_{0.1}O_{2.95}$ and $BaCe_{0.9}Yb_{0.1}O_{2.95}$ were investigated in atmospheres of H_2/H_2O/Ar, D_2/D_2O/Ar, and T_2/Ar.[§] The impedance spectra were analysed to resolve the bulk properties, and these were subjected to an Arrhenius analysis. The activation energies, shown in Fig. 3a, increased with isotope mass, except in the case of $BaCe_{0.9}Yb_{0.1}O_{2.95}$ in T_2/Ar, where it was abnormally low. In contradiction to most of the previous results, the difference $\Delta H_D - \Delta H_H$ was only 1.9 kJ mol^{-1} whereas a value of 4–5 kJ mol^{-1} was expected. The pre-exponentials, shown in Fig. 3b, decreased with increasing isotope mass, in accordance with the semi-classical theory, but contrary to the trends observed by Nowick et al. [15–17]. The tritium anomaly in ΔH_m could have been explained by poor isotope exchange, considering that T_2/Ar was used in preference to T_2/T_2O, had it not been for the consistent trends observed in the pre-exponentials. We hope that, despite the experimental difficulties in handling tritium, further work will be performed with this isotope, as well as with deuterium, in order to test the above discrepancies.

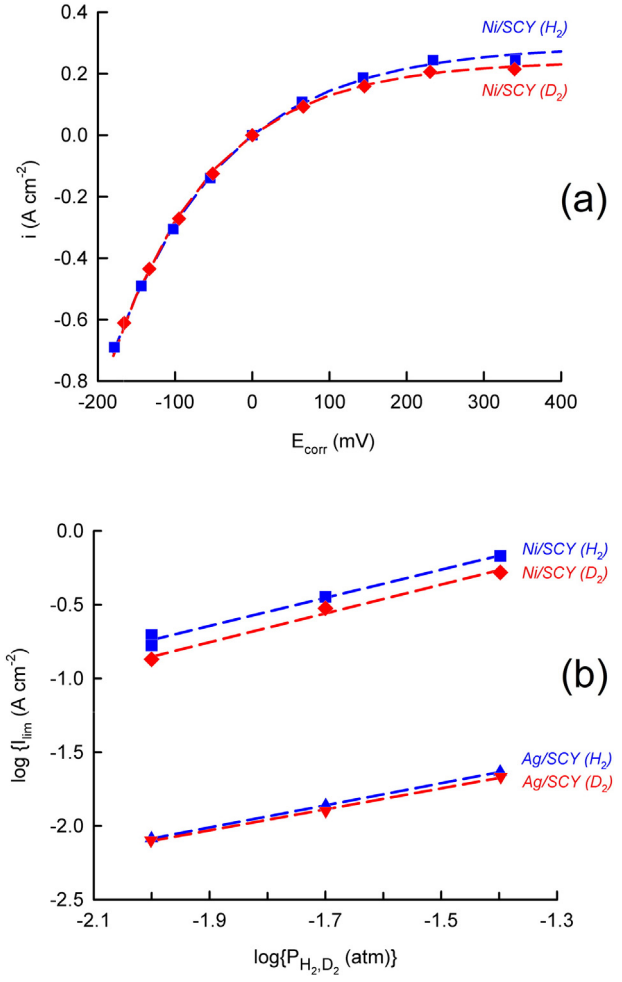

Fig. 4. Oxidation of hydrogen or deuterium on a metallic point contact electrode at 800 °C from Ref. [23]. (a) Current-potential curve for the oxidation of H_2 or D_2 diluted to 2% by volume in N_2 with a Ni electrode. (b) Dependence of anodic limiting currents on hydrogen/deuterium partial pressure in the oxidation of hydrogen/deuterium on a metallic point contact electrode for Ni and Ag electrodes.

2.3. Isotope effects in electrode kinetics

In comparison to the literature on bulk conductivity, little has been published on the isotope effect in electrode kinetics [22,23]. The oxidation of hydrogen to protons involves steps of adsorption, dissociation, diffusion, and charge transfer as shown in Eq. (11), any of which could be rate determining.

$$H_2(g) \leftrightarrow \; H_{2,ad} \leftrightarrow 2H_{ad} \leftrightarrow 2H^+ + 2e^-. \tag{11}$$

In a study of electrochemical oxidation of hydrogen, point contact electrodes of Ag and Ni were used with the perovskite proton conductor $Sr_{0.995}Ce_{0.95}Y_{0.05}O_{2.975}$ [23]. Under anodic polarisation, mass transport limited currents were observed, according to Eq. (12):

$$i = i_{\lim}\left\{1 - e^{\left(\frac{-\eta\beta F}{RT}\right)}\right\} \tag{12}$$

where i_{lim} is the limiting current, η is the overpotential, and β is a parameter that in certain cases is related to the number of electrons taking part in the reaction.

The dependence of these currents on P_{H_2}, P_{D_2} could be described by a simple power law:

$$i_{\lim} = i^0\left(P_{H_2}\right)^q \tag{13}$$

[§] T_2O was not included in the T_2/Ar atmosphere due to considerations of radiological safety.

where i^0 is the limiting current in hydrogen at a pressure of 1 atm. and q is the reaction order.

As shown in Fig. 4a, a minor difference in the current voltage curves for oxidation of H_2 and D_2 on a Ni electrode could be explained by a difference in the limiting currents. Considering the limiting currents for different concentrations of H_2 and D_2 (Fig. 4b), a reaction order, of circa 1 was obtained as for Ni, while for Ag a value of 0.7 was determined. This lead to the suggestion that, for Ni, the rate determining step (RDS) was non-dissociative adsorption or surface diffusion of H_2, while for Ag, the RDS probably involved the hydrogen atom [23].

An analysis of the limiting currents in Arrhenius representation (not shown) produced values in the range of 60–132 kJ mol^{-1}. Since these currents were thermally activated, they could not be ascribed to gas phase diffusion, but instead must be due to bulk or surface diffusion. The activation energies were higher for Ag than for Ni, and also higher for D_2 than for H_2, but did not follow the systematic pattern observed with the protonic conductivities.

2.4. Thermodynamic isotope effect

Tsidilkovski [24] considered the concentrations of H, D or T in an HTPC in equilibrium with H_2O, D_2O, and T_2O vapour respectively. He pointed out that the difference in vibrational entropy between the vapour and solid phases influenced the Gibbs free energy of reaction (2) for the three isotopes. Tsidilkovski demonstrated that, for equivalent hydration conditions, the concentration ratio [D]/[H] increased at low temperatures and low degrees of saturation; at temperatures of interest for HTPCs, this ratio exceeded the value of 2. Considering Eq. (10), this means that the conductivity pre-exponential for a D_2O-exchanged HTPC would exceed that of an H_2O exchanged one, even allowing for the lower attempt frequency of the D species.

Considering the relevance of the thermodynamic isotope effect to conduction mechanisms in HTPCs, scant attention has been given to its experimental study. The present authors measured concentration isotherms of H and D in the system $Ba_3(Ca_{1.18}Nb_{1.82})O_{2-\delta}$ for H_2O and D_2O at 800 °C [25]. In Fig. 5, these are plotted against $P^{½}_{H_2O}$ or $P^{½}_{D_2O}$. For the low levels of humidity employed, the solids should be far from saturated in protons, and so follow Sieverts' law, i.e. a solubility proportional to $P^{½}_{H_2O}$ or $P^{½}_{D_2O}$ [26]. On that basis, the plots in Fig. 5 should be linear and should pass thorough the origin. The plots are indeed linear and show significant differences between the isotherms for the two isotopes, although, contrary to expectations, the lines do not pass through the origin. For the hydrogen isotherm, the results agree with those an earlier study of $Ba_3(Ca_{1.18}Nb_{1.82})O_{2-\delta}$ [27]. Further work is needed to test these trends for other HTPC materials and temperatures other than 800 °C.

2.5. Spontaneous emf in H_2/D_2 cell

Matsumoto and co-workers have considered an electrochemical cell with HTPC electrolyte supplied with H_2 and D_2 on opposite sides. This results in the generation of an emf, for which the D_2 side is positive with respect to the H_2 side [28,29]. The emf arises because H^+ and D^+ migrate in opposite directions through the electrolyte, their two partial currents cancelling. Since the mobilities of the two species are different, but their partial currents the same, the resulting I·R drops must be different, generating to a net emf across the cell. A theoretical expression for the emf has been published earlier [28,29]:

$$E_{th} = -\ln\left\{\frac{\left(2\mu_D^0-\mu_{D_2}^0\right)}{2F}-\frac{\left(2\mu_H^0-\mu_{H_2}^0\right)}{2F}\right\}+\frac{RT}{2F}\ln\left(\frac{p_{H_2}}{p_{D_2}}\frac{\gamma_D^2}{\gamma_H^2}\frac{u_D^2}{u_H^2}\right) \quad (14)$$

where μ_i^0 are the standard chemical potentials of the species i, γ_i are the activity coefficients, u_i are the mobilities, the subscripts H_2/D_2 refer to the gaseous species and H/D to the species in the oxide. R, T, and F have their usual meanings. Fig. 6 shows the second term of Eq. (14), for H_2/D_2 pressures of 1 atm, activity coefficients of unity and a mobility ratio of $\sqrt{2}$. Fig. 6 also includes experimental data obtained on such a cell with H_2/D_2 gases humidified at ambient temperature with H_2O/D_2O and a solid electrolyte of $CaZr_{0.9}In_{0.1}O_{2.95}$ (at the experimental conditions, $CaZr_{0.9}In_{0.1}O_{2.95}$ has a protonic transport number of close to unity). As pointed out by Matsumoto [28], the magnitude of the observed H_2/D_2 cell emf indicates that the first term of Eq. (14) is negative, implying, for $CaZr_{0.9}In_{0.1}O_{2.95}$, a higher solubility for D^+ than H^+. This conclusion is analogous to the one reached by Tsidilkovski for the thermodynamic isotope effect in a typical high temperature proton conductor, namely a higher solubility of D^+ than H^+. Considering this connection, perhaps the two effects should be treated by a unified theory.

It is remarkable that, for the same combination of atmospheres, H_2/H_2O on one side and D_2/D_2O on the other, roughly similar emfs are generated, and that the sign of the emf depends on the conduction process in the electrolyte: D_2/D_2O negative for an oxide ion conductor and D_2/D_2O positive for a proton conductor. It is common for perovskite

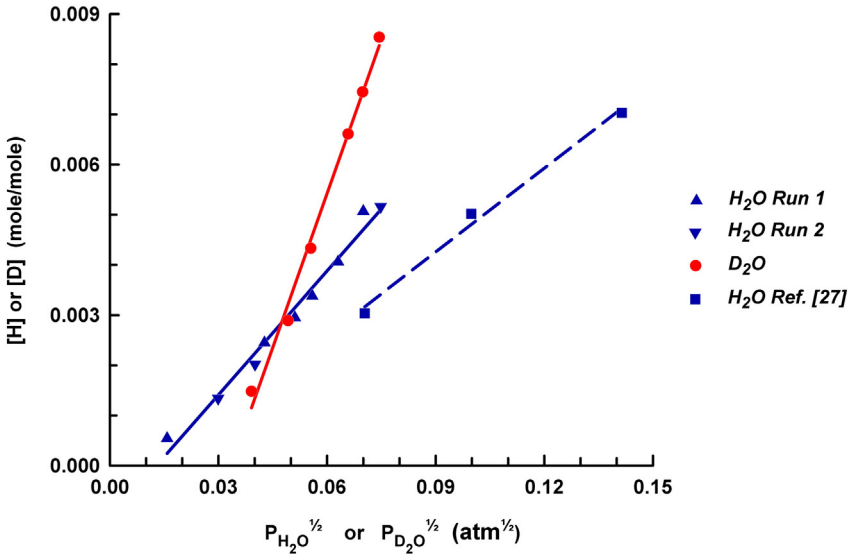

Fig. 5. Concentration isotherms for [H] and [D] in $Ba_3(Ca_{1.18}Nb_{1.82})O_{2-\delta}$ at different partial pressures of H_2O and D_2O, at 800 °C [25], together with results for [H] from another study [27]. Plotting the concentrations versus $(PH_2O)^{½}$ linearizes the isotherm, such that, for low vapour pressure, the slope is $\sqrt{M_b K_w/2}$ [26].

Please cite this article as: N. Bonanos, et al., H/D isotope effects in high temperature proton conductors, Solid State Ionics (2015), http://dx.doi.org/10.1016/j.ssi.2015.03.028

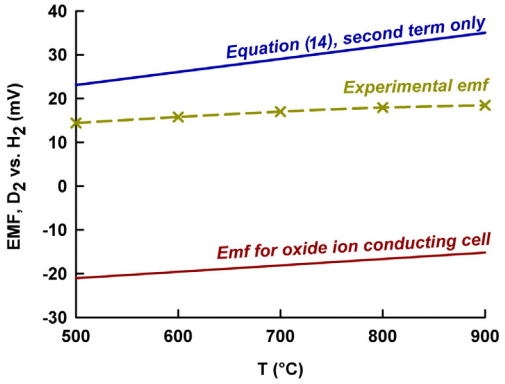

Fig. 6. Second term of Eq. (14) for the theoretical emf of a D_2/H_2 electrochemical cell plotted against temperature and the experimental emf obtained using the solid electrolyte $CaZr_{0.9}In_{0.1}O_{2.95}$ in Ref. [28]. The lower line is the theoretical emf for the corresponding cell with an oxide ion conductor (Eq. 1).

proton conductors to undergo a gradual transition from protonic to oxide ion conductivity at high temperatures, where the equilibrium of reaction (2) shifts to the left. Accordingly, the cell emf is expected to swing from positive to negative, passing through zero when the transport numbers of the two processes are equal.

Fig. 7 shows the response of two such cells for the perovskites $La_{0.7}Sr_{0.3}Sc_{0.8}Ti_{0.2}O_{2.95}$ (LSST) and $SrCe_{0.9}Y_{0.1}O_{2.95}$ (SCY), with emf cross-overs at 635 and 895 °C, respectively. In a separate study, the temperature at which the protonic transport number of LSST reached the value of 0.5 was somewhere in the region of 700 °C [30]. The corresponding temperature for SCY was slightly above 800 °C [31]. Thus, in principle, the H_2/D_2 cell emf can serve as a diagnostic experiment of the conduction mechanism, albeit a rather expensive one. It would be tempting to attempt to calibrate this method so that the curves in Fig. 7 could be converted to transport numbers, however this would be possible only if the polarisation resistances of the electrode processes for hydrogen/deuterium and for oxygen reactions were very small, an assumption that has been shown to be problematic [32].

3. Conclusions

The family of HTPCs shows a wealth of effects when the hydrogen in the solids is replaced by deuterium. These affect the infra-red spectra, the transport properties, H_2/D_2 oxidation kinetics, solubilities of H_2O/D_2O and the behaviour of H_2/D_2 cells with proton conducting electrolytes. In our opinion, the following are the most important points: 1) the concept of the classical harmonic oscillator is sufficient to explain the broad trends in the vibrational spectra. 2) This model does not hold for the transport properties, for which the semi-classical approach, or more advanced models, must be invoked. 3) Both the emf behaviour of H_2/D_2 electrochemical cells, and the thermodynamic isotope effect, demonstrate a higher solubility of D_2O than H_2O in these systems, but these effects have not yet been unified into a single theory. 4) H_2/D_2 cells can be used to diagnose the conduction mechanism in a solid electrolyte, as the polarity of the cell will be different for a proton conductor and for an oxide ion conductor.

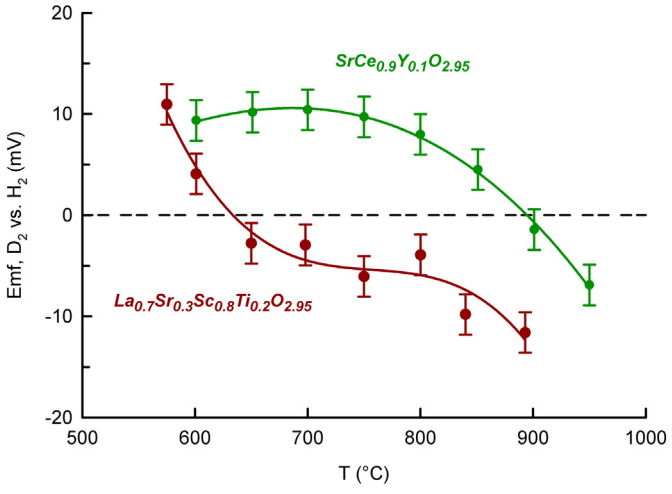

Fig. 7. Emfs of D_2/H_2 electrochemical cells for the perovskites $La_{0.7}Sr_{0.3}Sc_{0.8}Ti_{0.2}O_{2.95}$, described in Ref. [30], and $SrCe_{0.9}Y_{0.1}O_{2.95}$, in Ref. [31]. With increasing temperature, both systems display a transition from protonic to oxide ion conduction, concomitant with the cell emf approaching zero.

Acknowledgements

The authors acknowledge extensive contributions of their co-authors in previous publications, namely Mogens Mogensen, Marianne Glerup, Darja Kek, Charles Hatchwell, and Henrik Bentzer. They are also grateful for valuable discussions with Hiroshige Matsumoto, Vladislav Tsidilkovski, Yurii Baikov, and Christodoulos Chatzichristodoulou. N.B. thanks the FP7 project MetProCell FCH-JU 277916 Innovative Fabrication Routes and Materials for Metal and Anode Supported Proton Conducting Fuel Cells for financial support in attending SSPC-17. Some results obtained in this laboratory were generated within the project Advanced Ceramics for Protonics, funded by The New Energy Development Organisation (NEDO), Japan, in the period 1994 to 1997, and led by Prof. Hiroyasu Iwahara.

References

[1] David R. Lide (Ed.), CRC Handbook, 79th Edn.CRC Press 1998-99, p. 6.4.
[2] A.R. Ubbelohde, K.J. Gallagher, Acta Crystallogr. 8 (2) (1955) 71–83.
[3] M.W. Chase, et al., JANAF Thermochemical Tables3rd ed.vol. 1–2, Amer. Inst. of Physics Inc., New York, 1985.
[4] T. Norby, M. Widerøe, R. Glöckner, Y. Larring, Dalton Trans. 19 (2004) 3012–3018.
[5] K.-D. Kreuer, Annu. Rev. Mater. Res. 33 (1) (2003) 333–359.
[6] N. Bonanos, Solid State Ionics 145 (2001) 265–274.
[7] I. Kosacki, H.L. Tuller, Solid State Ionics 80 (3) (1995) 223–229.
[8] S. Ricote, G. Caboche, O. Heintz, J. Appl. Electrochem. 39 (4) (2009) 553–557.
[9] Y.M. Baikov, Solid State Ionics 97 (1) (1997) 471–476.
[10] N. Bonanos, F.W. Poulsen, J. Mater. Chem. 9 (1999) 431–434.
[11] N. Bonanos, in: R. Savinell, K. Ota, G. Kreysa (Eds.), Encyclopedia of Applied Electrochemistry, Springer-Verlag, Berlin, Heidelberg 2014, pp. 1514–1520.
[12] A. Potier, in: P. Colomban (Ed.), Proton Conductors: Solids, Membranes and Gels — Materials and Devices, Cambridge University Press 1992, p. 6.
[13] P. Colomban, in: P. Colomban (Ed.), Proton Conductors, Solids, Membranes, Gels — Materials and Devices, Cambridge University Press 1992, p. 45.
[14] M. Glerup, F.W. Poulsen, R.W. Berg, Solid State Ionics 148 (2002) 83–92.
[15] W.-K. Lee, A.S. Nowick, L.A. Boatner, Solid State Ionics 18 (1986) 989–993.
[16] T. Scherban, Y.M. Baikov, E.K. Shalkova, Solid State Ionics 66 (1993) 159–164.
[17] A.S. Nowick, A.V. Vaysleyb, Solid State Ionics 97 (1997) 17–26.
[18] W. Münch, G. Seifert, K.-D. Kreuer, J. Maier, Solid State Ionics 86 (1996) 647–652.
[19] W. Münch, K.-D. Kreuer, G. Seifert, J. Maier, Solid State Ionics 136 (2000) 183–189.
[20] R.C.T. Slade, N. Singh, J. Mater. Chem. 1 (3) (1991) 441–445.
[21] R. Mukundan, E.L. Brosha, S.A. Birdsell, A.L. Costello, F.H. Garzon, R.S. Willms, J. Electrochem. Soc. 146 (6) (1999) 2184–2187.
[22] T. Hibino, K. Mizutani, H. Iwahara, J. Electrochem. Soc. 140 (1993) 2588–2592.
[23] D. Kek, N. Bonanos, Solid State Ionics 125 (1-4) (1999) 345–353.
[24] V.I. Tsidilkovski, Solid State Ionics 162 (2003) 47–53.
[25] J.M. Huijser, Isotope effects in proton conducting oxides, M.Sc. Project Report, Materials Research Department, Risø National Laboratory, Roskilde, Denmark, 2003.
[26] A.S. Nowick, Solid State Ionics 77 (1995) 137–146.
[27] F. Krug, T. Schober, Solid State Ionics 92 (3-4) (1996) 297–302.
[28] H. Matsumoto, K. Takeguchi, H. Iwahara, J. Electrochem. Soc. 146 (4) (1999) 1486–1491.
[29] H. Matsumoto, H. Hayashi, T. Shimura, H. Iwahara, T. Yogo, Solid State Ionics 161 (2003) 93–103.
[30] C. Hatchwell, N. Bonanos, M. Mogensen, Solid State Ionics 162–163 (2003) 93–98.
[31] H.K. Bentzer, Development of Materials for Hydrogen Permeable Membranes(Ph.D. Thesis) Technical University of Denmark, 2010.
[32] H.K. Bentzer, N. Bonanos, J.W. Phair, Solid State Ionics 181 (3-4) (2010) 249–255.